



Published in final edited form as:

J Thorac Imaging. 2019 September ; 34(5): 313–319. doi:10.1097/RTI.0000000000000334.

Assessment of interstitial lung disease using lung ultrasound surface wave elastography – a novel technique with clinicoradiologic correlates

Ryan Clay, MD¹, Brian Bartholmai, MD², Boran Zhou, PhD², Ron Karwoski, BA⁴, Tobias Peikert, MD¹, Thomas Osborn, MD³, Srinivasan Rajagopalan, PhD², Sanjay Kalra, MD¹, Xiaoming Zhang, PhD²

¹Department of Pulmonary and Critical Care Medicine, Mayo Clinic, Rochester, MN 55905

²Department of Radiology, Mayo Clinic, Rochester, MN 55905

³Department of Rheumatology, Mayo Clinic, Rochester, MN 55905

⁴Department of Physiology and Biomedical Engineering, Mayo Clinic, Rochester, MN 55905

Abstract

Introduction—Optimal strategies to detect early interstitial lung disease (ILD) are unknown. ILD is frequently subpleural in distribution and affects lung elasticity. Lung Ultrasound Surface Wave Elastography (LUSWE) is a noninvasive method of quantifying superficial lung tissue elastic properties. In LUWSE a handheld device applied at the intercostal space vibrates the chest at a set frequency and the lung surface wave velocity is measured by an ultrasound probe 5mm away in the same intercostal space. We explored LUWSE's ability to detect ILD and correlated LUSWE velocity with physiologic, quantitative and visual radiologic features subjects with known ILD and healthy controls.

Methods—77 subjects with ILD, most due to connective tissue disease, and 19 healthy controls were recruited. LUSWE was performed on all subjects in 3 intercostal lung regions bilaterally. Comparison of LUSWE measures pulmonary function testing, visual assessment and quantitative analysis of recent CT imaging with Computer-Aided Lung Informatics for Pathology Evaluation and Rating (CALIPER) software.

Results—Sonographic velocities were higher in all lung regions for cases, with the greatest difference in the lateral lower lung. Median velocity in m/s was 5.84 vs 4.11 and 5.96 vs. 4.27 ($p < 0.00001$) for cases vs. controls, left and right lateral lower lung zones, respectively. LUSWE velocity correlated negatively with vital capacity and positively with radiologist and CALIPER-detected interstitial abnormalities.

Conclusion—LUSWE is a safe and noninvasive technique that showed high sensitivity to detect ILD and correlated with clinical, physiologic, radiologic and quantitative assessments of ILD. Prospective study in detecting ILD is indicated.

Keywords

Connective tissue disease-related interstitial lung disease (CT-ILD); ILD screening; Lung ultrasound; Lung ultrasound surface wave elastography

Introduction

Despite difference in clinical course between connective-tissue disease related interstitial lung disease (CTD-ILD) and idiopathic pulmonary fibrosis (IPF), interstitial lung diseases (ILD) tend to be progressive and irreversible.^{1,2} Epidemiologic study suggests that preclinical asymptomatic ILD exists, but time from initial development of disease to symptom onset may be years.³ While patients and treating clinicians hope for improvement, a realistic therapeutic goal is often slowing or arresting disease progression.⁴⁻⁶ Due to current limitations in medical therapy, the optimal window to intervene is likely at this pre-clinical stage. However, the best way to screen for pre-clinical ILD has yet to be determined. High-resolution computed tomographic (HRCT) is commonly used for the detection and characterization of pulmonary disease, but is generally not used to screen for asymptomatic ILD due to cost, radiation exposure and a high prevalence of incidental findings.^{1,7,8}

Ultrasound is widely available and has become an indispensable tool in the point-of-care management of pleural disease.⁹ Ultrasound's utility in pulmonary disease beyond the pleural cavity, however, is limited due to poor sonographic penetration through air. However ILDs, especially CTD-ILD and IPF, have a dominantly subpleural distribution,¹⁰⁻¹² and thoracic ultrasound can detect interstitial lung abnormalities, which show visually as the comet artifact – also known as B-lines. Unfortunately, B lines are a nonspecific finding and can be seen in any parenchymal or interstitial lung process including atelectasis and pulmonary edema. The detection and quantification of B-lines are operator-dependent, and the optimal approach and patient positioning is unknown.^{13,14} Varying scoring systems have been proposed to stratify disease severity in ILD with ultrasound based on B-lines, but none are standardized,¹⁵ and interpretation is dependent on subjective assessment and expertise.

The development of Lung Ultrasound Surface Wave Elastography has been previously detailed.^{16,17} Lung fibrosis – the final common pathway in varying ILDs – results in stiffened lung tissue. The velocity of sound wave propagation increases with tissue stiffness. In LUSWE an ultrasound probe measures the velocity of applied harmonic vibration through the surface lung tissue. A small pilot study showed clear differences in LUSWE velocity between subjects with ILD and healthy volunteers.¹⁷ We therefore hypothesized that LUSWE should have distinctly higher velocities in subjects with ILD when compared to healthy volunteers. We explored a structured approach to LUSWE in clinical practice to gain better understanding regarding its operating characteristics, sensitivity and specificity for detection of ILD. We compared the LUSWE measurements with pulmonary function testing (PFT), expert-applied clinical severity scores, thoracic radiologist visual assessment and quantitative CT analysis of the ultrasound footprint using validated CT post-processing software (CALIPER)¹⁸⁻²⁰ to explore the clinical relevance of this novel technique as both a screening and assessment tool of ILD. Elucidation of LUSWE characteristics and correlation

with currently accepted clinical features of disease are essential to its development as a proposed screening tool in patients at risk for ILD.

Methods

Patient recruitment

77 subjects with known interstitial lung disease and 19 never-smoker healthy controls were recruited to undergo LUSWE. All subjects had pulmonary function testing done within 12 months of LUSWE assessment. All radiologic and physiologic testing in the ILD group was performed for ongoing clinical care. Controls were verified to have normal pulmonary function testing, no significant exposures and a prior volumetric HRCT for research purposes within the prior 12 months. HRCT was assessed by CALIPER software and given a visual assessment severity score by a thoracic radiologist (BJB).¹⁸ Overall clinical severity was scored based on PFT results (SK). LUSWE results were not available to clinical care providers and therefore not used to make clinical decisions. This study was approved by the Mayo Clinic Institutional Review Board (IRB number 7-006863). All subjects provided informed consent.

Ultrasound surface wave elastography technique

Patients were tested sitting upright. The handheld shaker (FG-142, Labworks Inc, Costa Mesa, CA) was firmly applied to the skin with a force less than 1 Newton (Figure 1). The device has a 3mm footprint at the skin, and most subjects reported feeling mild vibration, but no discomfort. A 0.1 s harmonic excitation was generated at three separate frequencies: 100 Hz, 150 Hz and 200 Hz, with 3 measurements made each time using the Verasonics ultrasound system with the L11-4 ultrasound transducer (Verasonics Inc, Kirkland, WA) at the 6.4 MHz frequency. The transducer probe was placed 5mm away from the handheld shaker in the same intercostal space on the skin with firm gentle pressure using water-based transmission gel.

Each measurement was taken during breath hold at full inspiration. Three intercostal spaces were systematically recorded at each lung for a total of six measured interspaces per subject: the second intercostal space at the mid-clavicular line (upper anterior), one intercostal space above the diaphragm in the mid-axillary line (lower lateral) and one intercostal space above the diaphragm in the mid-scapular line (lower posterior). Ultrasound visualization was used to confirm each location and make fine adjustments as warranted by variations in subject anatomy. Total testing time per subject to accommodate all measurements was approximately 30 minutes.

Clinical scoring

All subjects had pulmonary function testing within 12 months of LUSWE assessment. Clinical severity scores were assessed based on impairment noted in the pulmonary function testing and assigned a grade from 0 – 3 where 0 = no impairment, 1 = mild, 2 = moderate and 3 = severe based on the worst of the percentage predicted TLC, DLCO or forced vital capacity (FVC) measurements, by an experienced pulmonologist (SK). All controls were

assigned a clinical severity score of 0 given that normal PFTs without symptoms were prerequisites for enrollment into the control group.

Radiologist visual scoring

71 subjects had visual assessment of their CT chest by an experienced thoracic radiologist (BB) and were assigned a score from 0 – 3 where 0 = no detected disease, 1 = mild disease, 2 = moderate disease and 3 = severe disease based on their most recent clinical chest CT.

CALIPER assessment

Computer Aided Lung Informatics for Pathology Evaluation and Rating (CALIPER) is a validated quantitative HRCT analysis tool developed at Mayo Clinic (CALIPER LTA, Imbio LLC, Minneapolis, MN) that reliably detects and quantifies parenchymal lung features. CALIPER features have been shown to correlate with radiologist visual assessment and pulmonary function testing.^{21,22} CALIPER has been validated in multiple studies to provide valuable prognostic data in ILD and to correlate well with physiologic metrics.²¹⁻²⁴

If available, a noncontrast volumetric HRCT within 12 months of LUSWE assessment was analyzed by CALIPER (54 cases, 19 controls) and the percentage of each CALIPER-detected lung tissue type was calculated. To correlate with the area of lung assessed by a projected footprint of the ultrasound transducer, the CALIPER characteristics in 6 discrete 15mm diameter hemispheres corresponding to the right and left lung upper anterior, lower lateral and lower posterior LUSWE evaluation locations were analyzed. CALIPER analysis was also performed on the entire lung volumes. Results were reported as percent of each lung tissue type present in the volume analyzed. The category interstitial lung abnormality (ILA) was a summed category of ground glass + reticular density + honeycomb cyst. The category ‘normal’ was generated by combining the tissue types of normal and mild low attenuation which correlate highly with normal parenchymal appearance and physiology in our own healthy controls and prior studies.^{20,25} The remaining moderate and severe low attenuation areas would generally correlate with areas of emphysema or hyperinflation, but there was little to none of these features in either ILD or control subjects and these measures were not used in our analysis.¹⁹

Statistical analysis

Categorical data were compared by chi square and continuous data by Wilcoxon Rank Sum with the exception of normally-distributed demographic data that was compared by paired t test. P values < 0.05 were considered significant; all tests were 2-tailed when applicable. Correlations between variables were assessed with r squared and analysis of variance. Univariate and multivariate analysis was done by nominal logistic regression. Data analysis was completed in JMP pro version 10.0 (Cary, NC, United States).

Results

77 subjects with interstitial lung disease and 19 healthy subjects were recruited to undergo a structured LUSWE exam. Diagnoses represented were scleroderma, n = 30 (39%); various other connective tissue diseases, n = 11 (14%); rheumatoid arthritis, n =

9(12%); antisynthetase syndrome, n = 6 (8%); idiopathic pulmonary fibrosis, n = 5(7%); polymyositis, n = 4 (5%); Sjogren's syndrome, n = 3 (4%); and other diagnoses including unclassified ILD, interstitial pneumonia with autoimmune features,²⁶ inflammatory myopathy, systemic lupus erythematosus and microscopic polyangiitis, n = 9 (12%).

ILD cases were older (62.2 versus 45.2 years old, $p = 0.0001$) with a higher BMI (28.7 versus 25.7 kg/m², $p = 0.008$) compared to healthy controls. Cases had significantly more restricted spirometry when compared to controls (Table 1). Healthy controls had essentially normal lungs by quantitative CT analysis compared to cases, who had substantial global involvement with ILA as detected by CALIPER (0% versus 45.1%, $p < 0.0001$). Cases, as expected, had higher radiologic and clinical severity scores ($p < 0.0001$).

Lung ultrasound surface wave elastography

LUSWE velocities were significantly higher in all lung fields of subjects with ILD versus healthy controls (Table 2). The median velocities had the greatest difference between subjects with ILD and healthy controls in the lower lateral lung zones at the 200 Hz frequency – the site measured 1 intercostal space above the diaphragm at the mid-axillary line. For example, the right lower lateral LUSWE velocity at 200 Hz was 5.84 m/s (interquartile range (IQR) 5.15 - 6.63) for cases versus 4.11 m/s for controls (IQR 3.50 – 4.15), $p < 0.0001$. Velocities in the left lower lateral lung zone performed similarly at the 200 Hz frequency: 5.96 m/s (IQR 5.19 – 7.07) versus 4.27 m/s (IQR 4.03 – 4.67) for cases versus controls, $p < 0.0001$. Though all zones and frequencies were statistically distinct, this difference was attenuated at the 100 Hz and 150 Hz frequencies, and was less pronounced for the upper anterior and lower posterior lung zones.

CALIPER measures

CALIPER metrics demonstrated a basilar-prevalent distribution of ILA within the cases and increased presence of ground glass and reticular density in all lung zones when compared to controls ($p < 0.0001$). This difference was the greatest when examining the lower posterior lung zones ($p < 0.0001$ for both left and right lower posterior lung zones). Cases paradoxically had significantly more CALIPER-detected 'normal' lung in the upper lung zones measured when compared to healthy controls. ($p = 0.014$, 0.001 for right and left, respectively).

Clinical correlations of LUSWE

The difference between LUSWE-detected velocities in healthy controls versus cases with ILD was greatest in the right lower lateral lung zone at 200 Hz and the correlation between LUSWE and other clinico-radiologic measures was therefore analyzed for this area, using the measurements made at 200 Hz. Distributions were compared between ILD cases and controls for surface wave velocity, FVC percent predicted and percent ILA as detected by CALIPER (Figure 2). Median LUSWE velocity was weakly negatively correlated with FVC percent predicted ($R^2 = 0.06$, $p = 0.02$) (Figure 3) and was weakly positively correlated with % ILA in the affected lung zone ($R^2 = 0.13$, $p = 0.002$) (Figure 3). LUSWE velocity in the right lower lateral zone also positively correlated with overall % ILA detected ($R^2 = 0.27$, $p < 0.0001$). Median LUSWE velocity increased with increasing radiologist-assessed visual

severity scores: 4.1 m/s for a score of 0, 5.1 m/s for a score of 1, 5.9 m/s for a score of 2 and 6.0 m/s for a score of 3; $p < 0.0001$ (Figure 3). Median LUSWE velocity was higher for subjects with a clinical severity score ≥ 1 , but did not reliably increase with increasing clinical severity: 4.2 m/s for a score of 0, 5.9 for a score of 1, 6.0 for a score of 2 and 5.3 for a score of 3, $p < 0.0001$ (Figure 3). In univariate nominal logistic regression, LUSWE velocity was predictive of ILD presence with an area under the curve (AUC) of 0.94 and odds ratio (OR) 13.4 (95% CI 4.0-44.6) per 1 m/s increase in LUSWE velocity, $p < 0.0001$. Adjusting for age did not affect the statistical significance of LUSWE velocity ($p < 0.0001$), though age was also a significant predictor of ILD ($p = 0.01$). BMI did not affect LUSWE prediction of ILD in bivariate modeling in which LUSWE was significant ($p < 0.0001$) and BMI was not ($p = 0.19$). Univariate analysis of the other lung zones to predict ILD at 200Hz found AUCs of 0.92 for right upper anterior, 0.82 for right lower posterior, 0.92 for left upper anterior, 0.88 for left lower lateral, and 0.76 for left lower posterior. A binary cutoff of 4.53 m/s for the 200Hz probe in the right middle lung zone yielded a sensitivity of 92% and specificity of 89% for detecting ILD.

Discussion

Early recognition of interstitial lung disease may be desirable for early treatment initiation to prevent future disability. LUSWE shows promise as an easily-applied and quantifiable noninvasive measure of lung stiffness. Though there are clear distinctions in visual assessment of CT, CALIPER analysis of CT and pulmonary function testing for cases versus controls, a significant number of patients with clinical disease had normal PFTs or minimal abnormality as detected by CALIPER or visual radiologist assessment. Furthermore, a small number of normal controls had mild visually-detected ILA but normal quantitative CT analysis. This discordance suggests that visual or quantitative CT may perform better as confirmatory rather than screening test. Still, LUSWE velocity correlates with physiologic, radiologic and quantitative metrics (Figure 4).

While a useful marker to follow disease progression and assess clinical impact,²⁷ pulmonary function tests are insensitive, particularly in detecting mild or early disease, which we observed in our cohort as well.²⁸ HRCT is used to characterize ILD, but has higher cost, involves radiation exposure and often finds incidental abnormalities that may or may not be of significance.²⁹ As evidenced in our study, healthy controls can also have interstitial lung abnormalities with unclear clinical significance, raising the question of when these radiologic findings truly represent disease. Ultrasound is portable and can be applied in a point-of-care fashion at a fraction of the cost when compared to HRCT. LUSWE correlated more strongly with overall CALIPER-detected ILA rather than specific sites which may be due to sampling error.

Quantitative scoring of B lines in lung ultrasound has been proposed as a way to assess and follow ILD.^{14,30,31} However, this requires training, can be operator-dependent and numerous pulmonary processes including atelectasis and edema may mimic the sonographic appearance of pulmonary fibrosis.³¹ The application of ultrasound screening using B-lines to evaluate rheumatoid arthritis-associated ILD showed only a 28% positive rate in cases versus 7% positive rate in healthy controls³². As LUSWE yields quantifiable results – a velocity –

inter-observer variability is eliminated and an objective threshold-based measure can be used to optimize the sensitivity and specificity in a screening setting.

LUSWE was less sensitive for discriminating normal from abnormal lung at the apices. There was actually more 'normal' lung as quantitatively assessed in subjects with ILD at the upper lung zones when compared to healthy controls. This may reflect compensatory hyperinflation of the upper lung as a reaction to basilar-predominant fibrosis. This makes the argument that the lower lateral and lower posterior lung zones may be best to assess for the presence of ILD – supported by our findings. We chose the lower lateral lung zone due to better discrimination when compared to the other lung zones. Though the lower lung zones are subject to gravity-dependent atelectasis, our earlier work showed that LUSWE velocity may be slowed by atelectasis given that velocities were significantly higher at total lung capacity than at functional residual capacity.¹⁶ The right lung was found preferable to the left to determine diseased lung from healthy control, potentially due to compressive effects of the mediastinum. A full assessment of the thorax took nearly 30 minutes; however, if we scale this back to only one lung zone at one velocity, this would come down to approximately 2 minutes per assessment – easily integrated into a clinic visit.

Connective tissue disease has a high prevalence of ILD, as much as 7% to 50% when looking at rheumatoid arthritis, Sjogren's syndrome, systemic sclerosis and inflammatory myopathies.^{33,34} This high prevalence of disease easily justifies clinical screening and LUSWE offers a point-of-care noninvasive assessment that deserves further evaluation, both for its screening potential and for monitoring disease progression. Additionally, BMI did not appear to affect LUSWE utility, with the maximum BMI included in our study of 42 kg/m² – though this needs further validation.

With a small number of subjects, we have demonstrated that surface wave velocity increases with radiologic severity and correlates with quantitatively-assessed ILD. This raises the potential that assessment of lung stiffness could be longitudinally tracked to monitor progression of disease or response to therapy. To better determine the optimal threshold values and define the utility of point-of-care LUSWE for disease monitoring, further prospective study in a larger cohort of patients with known ILD, patients at risk of ILD, normal subjects and patients with other diseases such as heart failure, emphysema or other parenchymal abnormalities over a wide range of ages, BMI and other characteristics is needed.

Conclusion

Lung ultrasound surface wave elastography is a novel and quantifiable noninvasive test that reliably detects interstitial lung disease. It has the best operating characteristics when applied to the lower lateral lung at 200 Hz. Increased LUSWE velocity correlates with radiologic and physiologic abnormality. Given its predictive ability in detecting ILD, prospective evaluation of its ability to screen for ILD in at-risk patients and monitor disease progression is warranted.

Acknowledgments

Conflicts of Interest: This study is supported by NIH R01HL125234 from the National Heart, Lung, and Blood Institute. Statistical consultation for this project was supported by Grant Number UL1 TR000135 from the National Center for Advancing Translational Sciences (NCATS). Its contents are solely the responsibility of the authors and do not necessarily represent the official views of the NIH. A portion of Brian Bartholmai's effort for development and validation of the lung ultrasound surface wave elastography technique is funded by NIH grant R01HL124234. Brian Bartholmai and Mayo Clinic are entitled to royalties from CALIPER software, licensed to Imbio, LLC. Some of the CALIPER technology is patent pending.

References

1. Ley B, Collard HR, King TE Jr. Clinical course and prediction of survival in idiopathic pulmonary fibrosis. *Am J Respir Crit Care Med.* 2011; 183(4):431–440. [PubMed: 20935110]
2. Park JH, Kim DS, Park IN, et al. Prognosis of fibrotic interstitial pneumonia: idiopathic versus collagen vascular disease-related subtypes. *Am J Respir Crit Care Med.* 2007; 175(7):705–711. [PubMed: 17218621]
3. Araki T, Putman RK, Hatabu H, et al. Development and Progression of Interstitial Lung Abnormalities in the Framingham Heart Study. *Am J Respir Crit Care Med.* 2016; 194(12):1514–1522. [PubMed: 27314401]
4. King TE Jr, Bradford WZ, Castro-Bernardini S, et al. A phase 3 trial of pirfenidone in patients with idiopathic pulmonary fibrosis. *N Engl J Med.* 2014; 370(22):2083–2092. [PubMed: 24836312]
5. Richeldi L, du Bois RM, Raghu G, et al. Efficacy and safety of nintedanib in idiopathic pulmonary fibrosis. *N Engl J Med.* 2014; 370(22):2071–2082. [PubMed: 24836310]
6. Zamora AC, Wolters PJ, Collard HR, et al. Use of mycophenolate mofetil to treat scleroderma-associated interstitial lung disease. *Respir Med.* 2008; 102(1):150–155. [PubMed: 17822892]
7. National Lung Screening Trial Research T, Aberle DR, Adams AM, et al. Reduced lung-cancer mortality with low-dose computed tomographic screening. *N Engl J Med.* 2011; 365(5):395–409. [PubMed: 21714641]
8. Hunninghake GM, Hatabu H, Okajima Y, et al. MUC5B promoter polymorphism and interstitial lung abnormalities. *N Engl J Med.* 2013; 368(23):2192–2200. [PubMed: 23692170]
9. Mayo PH, Doelken P. Pleural ultrasonography. *Clinics in Chest Medicine.* 2006; 27(2):215–+. [PubMed: 16716814]
10. Wells AU, Hansell DM, Rubens MB, Cullinan P, Black CM, du Bois RM. The predictive value of appearances on thin-section computed tomography in fibrosing alveolitis. *Am Rev Respir Dis.* 1993; 148(4 Pt 1):1076–1082. [PubMed: 8214928]
11. Desai SR, Veeraraghavan S, Hansell DM, et al. CT features of lung disease in patients with systemic sclerosis: comparison with idiopathic pulmonary fibrosis and nonspecific interstitial pneumonia. *Radiology.* 2004; 232(2):560–567. [PubMed: 15286324]
12. Raghu G, Collard HR, Egan JJ, et al. An official ATS/ERS/JRS/ALAT statement: idiopathic pulmonary fibrosis: evidence-based guidelines for diagnosis and management. *Am J Respir Crit Care Med.* 2011; 183(6):788–824. [PubMed: 21471066]
13. Chichra A, Makaryus M, Chaudhri P, Narasimhan M. Ultrasound for the Pulmonary Consultant. *Clin Med Insights-Ci.* 2016; 10
14. Vassalou EE, Raissaki M, Magkanas E, Antoniou KM, Karantanas AH. Modified Lung Ultrasonographic Technique for Evaluation of Idiopathic Pulmonary Fibrosis: Lateral Decubitus Position. *J Ultrasound Med.* 2017; 36(12):2525–2532. [PubMed: 28656715]
15. Wang YK, Gargani L, Barskova T, Furst DE, Cerinic MM. Usefulness of lung ultrasound B-lines in connective tissue disease-associated interstitial lung disease: a literature review. *Arthritis Res Ther.* 2017; 19
16. Zhang X, Osborn T, Kalra S. A noninvasive ultrasound elastography technique for measuring surface waves on the lung. *Ultrasonics.* 2016; 71:183–188. [PubMed: 27392204]
17. Zhang X, Osborn T, Zhou B, et al. Lung Ultrasound Surface Wave Elastography: A Pilot Clinical Study. *IEEE Trans Ultrason Ferroelectr Freq Control.* 2017; 64(9):1298–1304. [PubMed: 28866480]

18. Bartholmai BJ, Raghunath S, Karwoski RA, et al. Quantitative computed tomography imaging of interstitial lung diseases. *J Thorac Imaging*. 2013; 28(5):298–307. [PubMed: 23966094]
19. Foley F, Raghunath S, Rajagopalan S, et al. Computer-Aided Lung Informatics For Pathology Evaluation And Rating (caliper) Analysis Of Chest CT To Detect Histologically Proven Emphysema. *American Journal of Respiratory and Critical Care Medicine*. 2016; 193
20. Jacob J, Bartholmai BJ, Rajagopalan S, et al. Automated Quantitative Computed Tomography Versus Visual Computed Tomography Scoring in Idiopathic Pulmonary Fibrosis: Validation Against Pulmonary Function. *J Thorac Imaging*. 2016; 31(5):304–311. [PubMed: 27262146]
21. Maldonado F, Moua T, Rajagopalan S, et al. Automated quantification of radiological patterns predicts survival in idiopathic pulmonary fibrosis. *Eur Respir J*. 2014; 43(1):204–212. [PubMed: 23563264]
22. Raghunath S, Rajagopalan S, Karwoski RA, et al. Quantitative stratification of diffuse parenchymal lung diseases. *PLoS One*. 2014; 9(3):e93229. [PubMed: 24676019]
23. Jacob J, Bartholmai BJ, Rajagopalan S, et al. Evaluation of computer-based computer tomography stratification against outcome models in connective tissue disease-related interstitial lung disease: a patient outcome study. *BMC Med*. 2016; 14(1):190. [PubMed: 27876024]
24. Jacob J, Bartholmai BJ, Rajagopalan S, et al. Mortality prediction in idiopathic pulmonary fibrosis: evaluation of computer-based CT analysis with conventional severity measures. *Eur Respir J*. 2017; 49(1)
25. Jacob J, Bartholmai BJ, Rajagopalan S, et al. Functional and prognostic effects when emphysema complicates idiopathic pulmonary fibrosis. *Eur Respir J*. 2017; 50(1)
26. Fischer A, Antoniou KM, Brown KK, et al. An official European Respiratory Society/American Thoracic Society research statement: interstitial pneumonia with autoimmune features. *Eur Respir J*. 2015; 46(4):976–987. [PubMed: 26160873]
27. Martinez FJ, Flaherty K. Pulmonary function testing in idiopathic interstitial pneumonias. *Proc Am Thorac Soc*. 2006; 3(4):315–321. [PubMed: 16738195]
28. Suliman YA, Dobrota R, Huscher D, et al. Brief Report: Pulmonary Function Tests: High Rate of False-Negative Results in the Early Detection and Screening of Scleroderma-Related Interstitial Lung Disease. *Arthritis Rheumatol*. 2015; 67(12):3256–3261. [PubMed: 26316389]
29. Jacobs PC, Mali WP, Grobbee DE, van der Graaf Y. Prevalence of incidental findings in computed tomographic screening of the chest: a systematic review. *J Comput Assist Tomogr*. 2008; 32(2): 214–221. [PubMed: 18379305]
30. Barskova T, Gargani L, Guiducci S, et al. Lung ultrasound for the screening of interstitial lung disease in very early systemic sclerosis. *Ann Rheum Dis*. 2013; 72(3):390–395. [PubMed: 22589373]
31. Dubinsky TJ, Shah H, Sonneborn R, Hippe DS. Correlation of B-Lines on Ultrasonography With Interstitial Lung Disease on Chest Radiography and CT Imaging. *Chest*. 2017; 152(5):990–998. [PubMed: 28522112]
32. Moazedi-Fuerst FC, Kielhauser SM, Scheidl S, et al. Ultrasound screening for interstitial lung disease in rheumatoid arthritis. *Clin Exp Rheumatol*. 2014; 32(2):199–203. [PubMed: 24642277]
33. Bongartz T, Nannini C, Medina-Velasquez YF, et al. Incidence and mortality of interstitial lung disease in rheumatoid arthritis: a population-based study. *Arthritis Rheum*. 2010; 62(6):1583–1591. [PubMed: 20155830]
34. Castelino FV, Varga J. Interstitial lung disease in connective tissue diseases: evolving concepts of pathogenesis and management. *Arthritis Res Ther*. 2010; 12(4):213. [PubMed: 20735863]

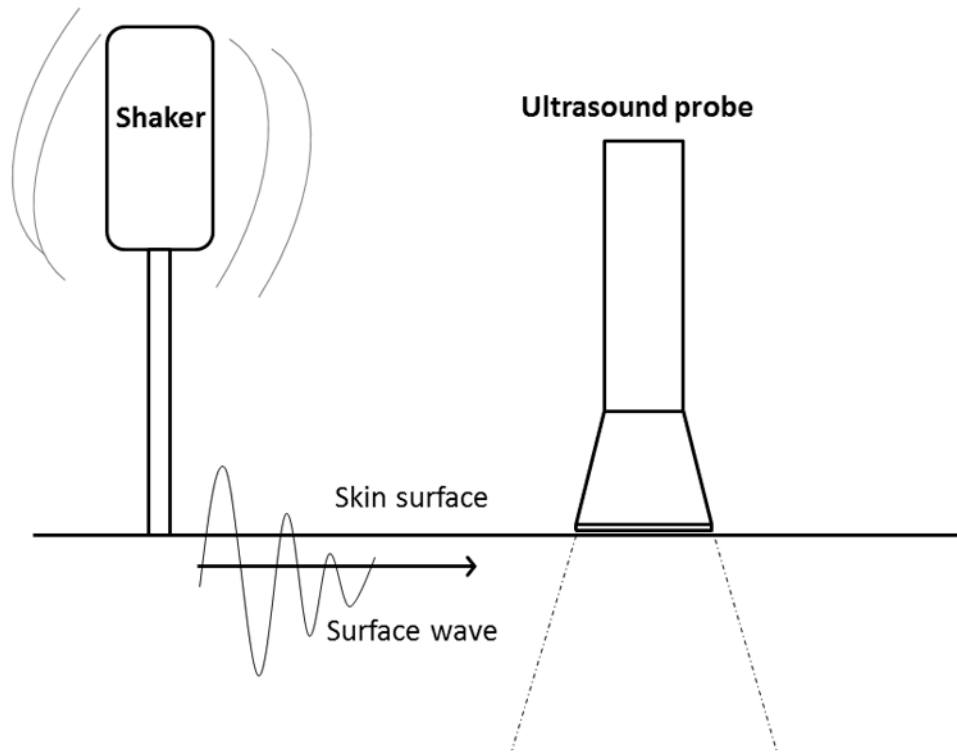


Figure 1. Cartoon depicting surface wave elastography. A handheld shaker is held firmly to the skin surface generating a surface wave that is detectable by an ultrasound probe held 5mm away to measure velocity in m/s.

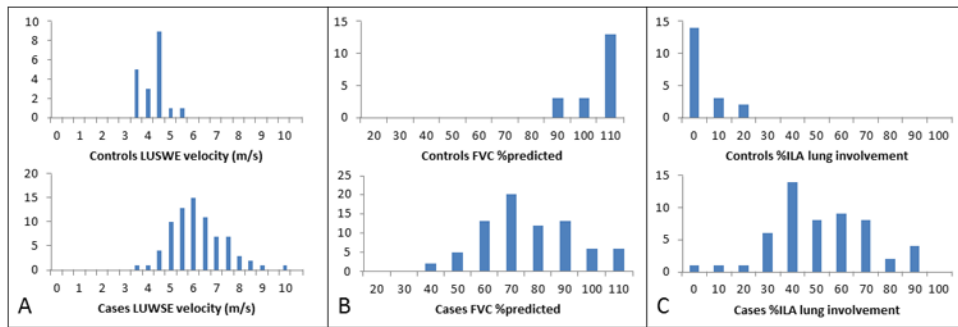


Figure 2. Distribution histograms for surface wave velocity for (a) ILD cases versus controls in the right lower lateral lung zone at 200 Hz (b) FVC percent predicted for ILD cases versus controls and (c) percent of CALIPER-detected ILA for ILD cases versus controls.

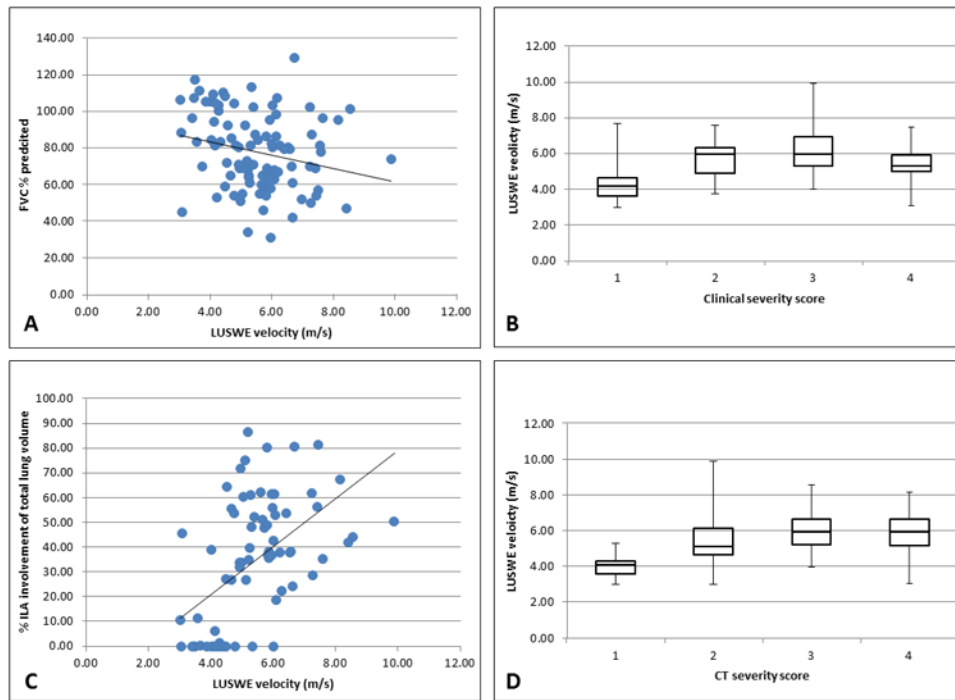


Figure 3.

Linear regression analysis shows a weak negative correlation between FVC % predicted and LUSWE velocity in (A) and a weak positive correlation between CALIPER-detected ILA and LUSWE velocity (C). Median analysis shows quintiles of LUSWE velocity by clinical severity score in (B) and by radiologist-assessed CT severity score (D). All velocities were measured in the right lower lateral lung zone.

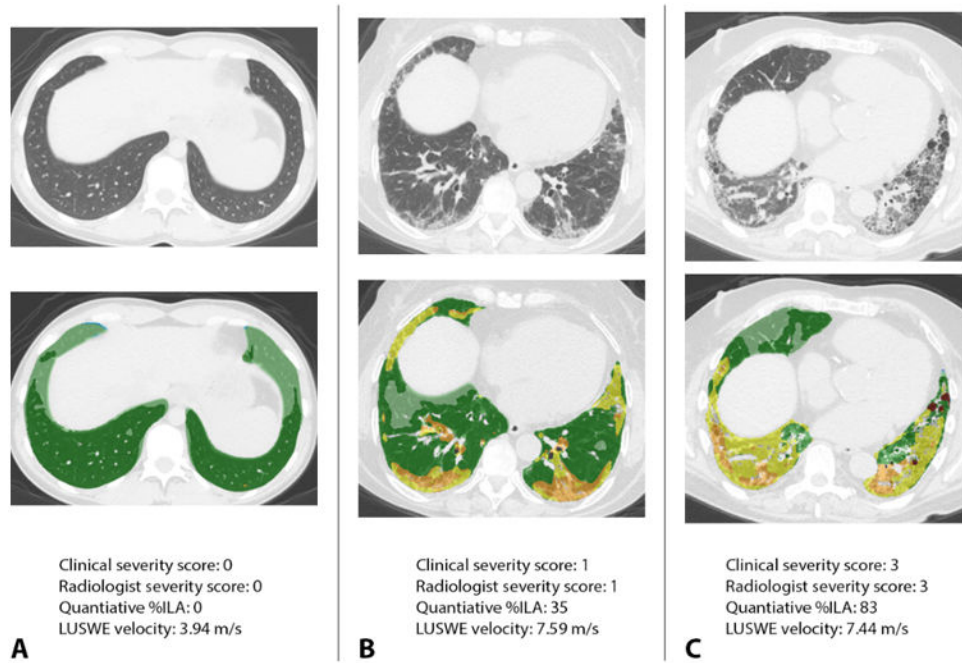


Figure 4.

Case examples of LUSWE velocity and radiologic appearance, quantitative analysis and clinical severity. Panel **A** demonstrates a healthy control with a normal CT chest and quantitatively normal lungs color-coded as green and light green by CALIPER. LUSWE velocity is substantially slower than diseased subjects at 3.94 m/s. Panel **B** depicts a subject with clinically and radiologically mild interstitial lung disease. Note foci of yellow and orange in the quantitatively analyzed scan depicting zones of interstitial lung abnormalities involving 35% of the total lung volume. The LUSWE velocity is significantly higher. Panel **C** shows a case with both high clinical and visually-assessed severity with diffuse disease involving 83% of the lung as quantitatively assessed, also demonstrating high LUSWE velocity.

Table 1

Age, BMI and pulmonary function testing presented as mean with standard deviation. CALIPER data presented as median with interquartile range. Two-tailed T tests and Wilcoxon Rank Sum tests were used to determine significance. Severity scores compared by chi square.

	Cases (n = 77)	Controls (n = 19)	P
Age	62.2 (\pm 13.4)	45.2 (\pm 15.1)	0.0001
BMI (kg/m ²)	28.7 (\pm 5.9)	25.7 (\pm 3.7)	0.008
Gender			0.39
M	34 (44%)	9 (47%)	
F	43 (56%)	10 (53%)	
FEV1 % predicted	73.9% (\pm 19.0)	102.5% (\pm 8.7)	<0.0001
FVC % predicted	72.1% (\pm 17.9)	102.4% (\pm 9.6)	<0.0001
FEV1/FVC	85.2 (\pm 11.4)	80.5 (\pm 4.9)	0.008
CALIPER			
Normal	51.9% (39.3 – 63.2)	93.5% (84.5 – 98.3)	<0.0001
Ground glass	34.5% (20.9 – 50.7)	0% (0 – 0)	<0.0001
Reticular	8.2% (3.0 – 13.6)	0% (0 – 0)	<0.0001
Honeycomb	0% (0 – 0.2)	0% (0 – 0)	0.001
ILA	45.1% (35.3 – 60.6)	0% (0 – 0)	<0.0001
Radiologic severity score			
0	0 (0%)	16 (84.2%)	<0.0001
1	19 (26.8%)	3 (15.8%)	
2	35 (49.3%)	0	
3	17 (23.9%)	0	
Clinical severity score			
0	4 (5.2%)	19 (100%)	<0.0001
1	15 (19.5%)	0	
2	39 (50.7%)	0	
3	19 (24.7%)	0	

Table 2

LUSWE velocities by lung zone in m/s. Data presented by median with interquartile range. P values calculated by Wilcoxon Rank Sum.

	Cases (n = 77)	Controls (n = 19)	P
Right upper anterior lung zone			
100 Hz	2.83 (2.44 – 3.18)	2.37 (2.25 – 2.74)	0.0004
150 Hz	4.31 (3.84 – 4.67)	3.18 (3.02 – 3.66)	<0.0001
200 Hz	5.82 (5.08 – 6.34)	4.40 (3.94 – 4.74)	<0.0001
Right lower lateral lung zone			
100 Hz	2.89 (2.51 – 3.07)	2.25 (2.16 – 2.50)	0.0001
150 Hz	4.28 (3.82 – 4.76)	3.43 (3.01 – 3.71)	<0.0001
200 Hz	5.84 (5.15 – 6.63)	4.11 (3.50 – 4.35)	<0.0001
Right lower posterior lung zone			
100 Hz	2.89 (2.51 – 3.12)	2.34 (2.28 – 2.92)	0.015
150 Hz	4.18 (3.81 – 4.67)	3.77 (3.48 – 4.00)	0.001
200 Hz	6.02 (5.29 – 7.05)	4.65 (4.06 – 5.41)	<0.0001
Left upper anterior lung zone			
100 Hz	2.77 (2.45 – 3.20)	2.38 (2.06 – 2.54)	0.0002
150 Hz	4.14 (3.74 – 4.72)	3.17 (2.71 – 3.55)	<0.0001
200 Hz	5.72 (5.02 – 6.37)	3.97 (3.69 – 4.43)	<0.0001
Left lower lateral lung zone			
100 Hz	2.90 (2.68 – 3.32)	2.32 (2.14 – 2.71)	<0.0001
150 Hz	4.51 (3.80 – 4.98)	3.23 (3.01 – 3.94)	<0.0001
200 Hz	5.96 (5.19 – 7.07)	4.27 (4.03 – 4.67)	<0.0001
Left lower posterior lung zone			
100 Hz	2.69 (2.32 – 3.25)	2.22 (1.99 – 2.62)	0.007
150 Hz	3.96 (3.40 – 4.51)	3.29 (3.14 – 3.84)	0.008
200 Hz	5.33 (4.67 – 6.15)	4.51 (3.77 – 5.02)	0.0004

Table 3

CALIPER characteristics by lung zone. Data presented as percent volume by median with interquartile range. P values calculated by Wilcoxon Rank Sum.

	Cases (n = 54)	Controls (n = 19)	P
Right upper anterior lung zone			
% ground glass	0% (0 – 3.6)	0% (0 – 0)	0.002
% reticular	0% (0 – 1.2)	0% (0 – 0)	0.003
% honeycomb	0% (0 – 0)	0% (0 – 0)	0.553
% ILA	0% (0 – 8.7)	0 (0 – 0)	0.001
% normal	99.9% (87.1 – 100)	90.3% (74.2 – 98.9)	0.014
Right lower lateral lung zone			
% ground glass	24.9% (5.3 – 66.1)	0% (0 – 0)	<0.0001
% reticular	3.1% (0.5 – 10.2)	0% (0 – 0)	<0.0001
% honeycomb	0% (0 – 0)	0% (0 – 0)	0.04
% ILA	38.3% (9.6 – 81.4)	0% (0 – 0)	<0.0001
% normal	59.9% (18.6 – 87.2)	99.9% (97.0 – 100)	<0.0001
Right lower posterior zone			
% ground glass	67.7% (34.1 – 91.8)	0% (0 – 0)	<0.0001
% reticular	9.5% (0.3 – 32.4)	0% (0 – 0)	<0.0001
% honeycomb	0% (0 – 0)	0% (0 – 0)	0.133
% ILA	97.2% (72.3 – 99.9)	0 (0 – 0)	<0.0001
% normal	2.9% (0.1 – 27.8)	100% (92.0 – 100)	<0.0001
Left upper anterior lung zone			
% ground glass	0% (0 – 4.3)	0% (0 – 0)	0.001
% reticular	0% (0 – 3.1)	0% (0 – 0)	0.001
% honeycomb	0% (0 – 0)	0% (0 – 0)	0.298
% ILA	0% (0 – 17.1)	0% (0 – 0)	0.0009
% normal	95.9% (79.7 – 100)	85.6% (69.8 – 95.3)	0.046
Left lower lateral lung zone			
% ground glass	38.1% (12.5 – 72.3)	0% (0 – 0)	<0.0001
% reticular	3.0% (1.0 – 7.0)	0% (0 – 0)	<0.0001
% honeycomb	0% (0 – 0)	0% (0 – 0)	0.08
% ILA	62.7% (19.1 – 85.2)	0% (0 – 0)	<0.0001
% normal	37.2% (14.7 – 80.9)	100% (94.7 – 100)	<0.0001
Left lower posterior lung zone			
% ground glass	67.1% (33.3 – 88.4)	0% (0 – 0)	<0.0001
% reticular	12.9% (1.8 – 25.8)	0% (0 – 0.3)	<0.0001
% honeycomb	0% (0 – 0)	0% (0 – 0)	0.226
% ILA	96.0 (70.1 – 100)	0 (0 – 0.3)	<0.0001

	Cases (n = 54)	Controls (n = 19)	P
% normal	4.0% (0 – 29.4)	99.7% (92.8 – 100)	<0.0001

Author Manuscript

Author Manuscript

Author Manuscript

Author Manuscript